Resource recovery of cupola dust: Study on sorptive property and mechanism for hydrogen sulfide

T. HATTORI
Department of Environmental Chemistry and Materials, Faculty of Environmental Science and Technology, Okayama University, Tsushima-Naka, Okayama, 700-8530, Japan; New Business Division, Aisin Takaoka Co., LTD., Tennoh, Takaokashin-Machi, Toyota, 473-8501, Japan

M. MATSUDA, M. MIYAKE*
Department of Environmental Chemistry and Materials, Faculty of Environmental Science and Technology, Okayama University, Tsushima-Naka, Okayama, 700-8530, Japan
E-mail: mmiyake@cc.okayama-u.ac.jp

Published online: 21 April 2006

Properties and mechanism for sorption of hydrogen sulfide (H_2S) by cupola dust, which is formed by the solidification of gas exhausted from cupola furnaces, have been investigated through the characterizations, aiming at recycling as the desulfurization. From the results, the sorptive property was found to be induced by spinel-type crystals such as $(Mn_xZn_{1-x})(Mn_yFe_{1-y})_2O_4$ solid solutions in spherical matrixes comprising of amorphous SiO_2 at room temperature in existence of water vapor. The further examination on the spinel-type crystals extracted by NaOH treatments revealed that H_2S was dissolved in water adsorbed on the surface of the spinel-type crystals, and reacted with metal ions released from them. In addition, the H_2S sorptive property was indicated to depend on amounts of Mn and Zn in the spinel-type crystals.

1. Introduction

Treatment of waste is one of the key elements in ensuring a sustainable environment. Substantial research is continuing in the area of recovering general and industrial wastes as resources. For example, wastes containing Si and Al such as waste incineration fly ash [1–3], coal fly ash [4–11], etc. are converted into zeolitic compounds, and used as raw materials for making cement [12].

Cupola dust, which is formed by the solidification of gas exhausted from cupola furnaces in steel industries or foundries, has fallen behind in terms of resource recovery, in spite of its containing useful transition elements. Thus, as over hundreds of thousands of tons of the cupola dust per year are landfilled in Japan, our investigation has been conducted to find the most effective reuse of the cupola dust. Consequently, the following were found; the dust possesses a good removal property for poisonous gases, especially for hydrogen sulfide (H_2S), and furthermore, this property is induced by spinel nanocrystals with 10–50 nm in dimension such as $(Mn_xZn_{1-x})(Mn_yFe_{1-y})_2O_4$ solid solutions in spherical matrixes comprising of amorphous SiO_2, as shown in Fig. 1 [13].

Other researchers have investigated the performance of spinel-type crystals for sorbing H_2S from hot coal gas under reduction condition, and discussed the desulfurization [14–17]. The reduction condition causes the spinel-type crystals to decompose into the constituent metal oxides, which act as desulfurization sorbents. Compared with their results, the sorptive mechanism for H_2S by the spinel-type nanocrystals in the dust seems different, because the H_2S sorption of the dust occurs at room temperature. In this paper, we report the performance of the spinel-type nanocrystals in the dust for sorbing H_2S at room temperature, and discuss the sorptive mechanism.

2. Experimental

2.1. Materials

Metal vapor exhausted from a cupola furnace is solidified through the cooling system interconnected to the top of the cupola furnace, and the solidified particles, which we call cupola dust, are trapped by the bag filter. Three lots of cupola dust, which were collected from the bag filter in the plant of Aisin Takaoka Co. Ltd. (Toyota, Japan) on different days, were employed in this work.

*Author to whom all correspondence should be addressed.
0022-2461
DOI: 10.1007/s10853-006-6223-6

2.2. Analysis

Chemical composition of the dust was analyzed by an X-ray fluorescence (XRF) technique on a Rigaku RIX3000 spectrometer (Tokyo, Japan). The crystalline phases in the dust were identified by powder X-ray diffraction (XRD), using a Rigaku RINT2100/PC diffractometer with monochromated CuKα radiation (Tokyo, Japan). Microstructures of the dust were observed by a Hitachi HF-2000 transmission electron microscope (TEM; Tokyo, Japan) operated at 200 kV. The specific surface area of the dust was estimated by nitrogen adsorption isotherm measurement with the BET method, using a BEL-Japan BELSORP18 instrument (Osaka, Japan).

2.3. H_2S sorption

Removal amounts of the dust for H_2S gas were measured by the gravimetric method using a quartz spring balance set in a glass tube (ca. 2 dm^3) connected to a vacuum line. The dust of 0.1 g was dried at 303 K under vacuum lower than 5 Pa in a glass tube, and then water vapor was fed into the glass tube, because the H_2S sorption does not occur in dry circumstances. The relative water vapor pressure (P/P_0; P is equilibrium pressure and P_0 saturation pressure) was controlled at about 0.6, referring to the mean humidity in the air. The weights of dry dust under vacuum and wet dust after reaching equilibrium were measured. After the measurements, pure H_2S gas of 20 kPa was fed into the glass tube. The weight of H_2S sorbed on the wet dust was measured after 24 h. The net weight of sorbed H_2S per 1 g of the dry dust was regarded as an H_2S sorption capacity. Furthermore, P/P_0 was changed from 0 to 0.92 to examine the influence of water on the H_2S sorptive property of the dust.

2.4. Hydrothermal treatment

The dust was hydrothermally treated in the presence of 5–15 M (mol · dm^{-3}) NaOH (special grade; Kanto, Tokyo Japan) solutions. The solid/liquid ratios were set at 1/30–1/4. The treatments were performed at 353–398 K for 4.5–41 h in a Teflon-lined autoclave under an autogeneous pressure with continuous stirring. The products after the treatment were filtered, and repeatedly washed with deionized water. The resulting materials were dried at 333 K for 24 h, and ground for further analyses, i.e. XRF and XRD analyses, measurements of H_2S sorptive capacity, solubility, etc.

2.5. Solubility

NaOH-treated cupola dust of 0.2 g was dispersed into deionized water of 25 ml in a sample vessel. The vessel was set in a shaker and shaken at 200 rpm for 20 h. Then, the suspension was filtered, and the filtrate was analyzed for Fe, Zn and Mn by Inductively Coupled Plasma (ICP), using a Shimadzu ICP-5000 (Kyoto, Japan). The total concentration of Fe, Zn and Mn was regarded as a solubility of the NaOH-treated dust.

TABLE I Chemical composition of cupola dusts

	Content (mass%)		
Component	lot 1	lot 2	lot 3
O	39.5	42.6	42.8
Mg	0.5	0.7	0.7
Al	2.2	1.7	1.4
Si	15.5	17.8	14.8
P	0.1	0.1	0.1
S	0.3	0.3	0.4
K	1.3	1.1	0.9
Ca	4.1	3.0	2.1
Mn	7.8	6.9	5.3
Fe	11.8	12.6	11.7
Zn	15.3	11.9	18.1
Sn	0.1	0.1	0.1
Pb	> 0.4	0.3	0.3

3. Results and discussion

3.1. Structure and composition

Chemical compositions of lot 1–3 dusts analyzed by an XRF technique are listed in Table I, and XRD patterns of three lots are illustrated in Fig. 2. Though amounts of metals in each lot showed some differences, the XRD patterns were similar to one another. The main crystalline phase in the dust was identified as a spinel-type compound, accompanied by small amounts of Fe_2O_3, Zn_2SiO_4 and quartz. The spinel-type compound, which forms nanocrystals, as seen in Fig. 1, is mainly a substitutional solid solution of $ZnFe_2O_4$, where both the M^{II} and M^{III} sites are partly occupied by Mn, i.e., $(Mn_xZn_{1-x})(Mn_yFe_{1-y})_2O_4$ solid solutions, according to our previous work by TEM [13].

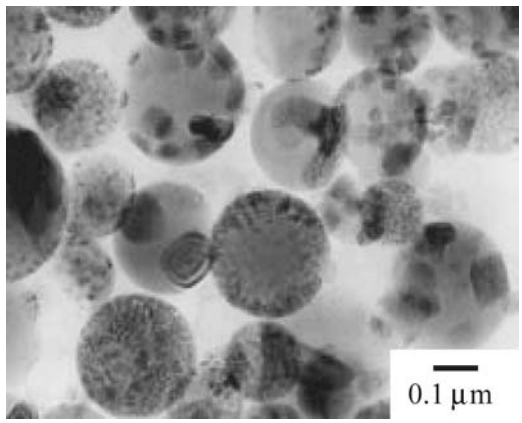

Figure 1 TEM image of lot 1 dust. Opaque particles and translucent spherical-shaped matrixes are spinel-type nanocrystals and amorphous SiO_2, respectively.

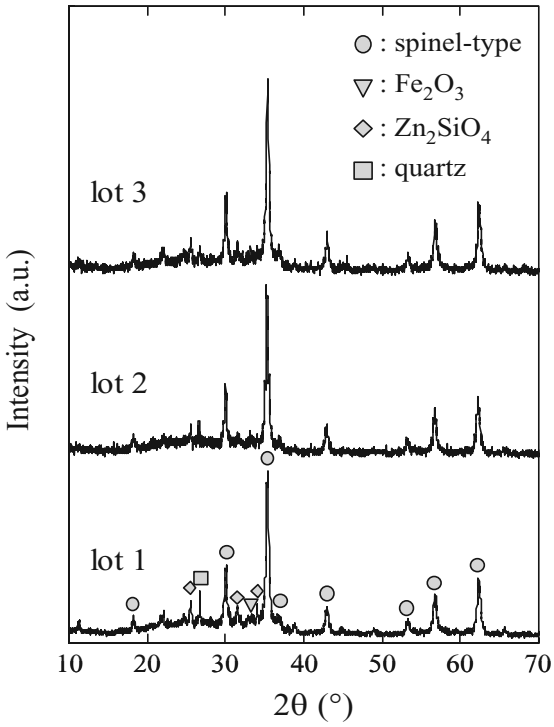

Figure 2 XRD patterns of lot 1–3 dusts.

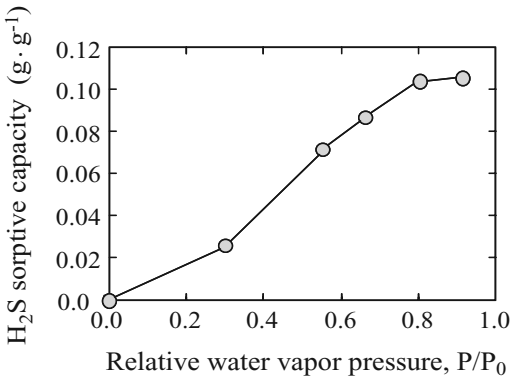

Figure 3 H_2S sorptive capacity of lot 1 dust as a function of relative water vapor pressure, P/P_0.

3.2. Sorptive property

The dust was not able to remove H_2S in dry circumstances through our examining the H_2S sorptive properties. Then, the correlation between the relative water vapor pressure and the H_2S sorptive property was checked. As shown in Fig. 3, the H_2S sorptive capacity of the dust increased with increasing water vapor pressure in the glass tube. An amount of water adsorbed on the dust also increased with increasing water vapor pressure. From these results, the water adsorbed on surface of the dust was considered to play an important role as a sorptive field.

3.3. Extraction of spinel-type nanocrystals

The dust was hydrothermally treated in the presence of NaOH solutions to extract the spinel-type nanocrystals, because they are in the amorphous SiO_2 matrixes. First,

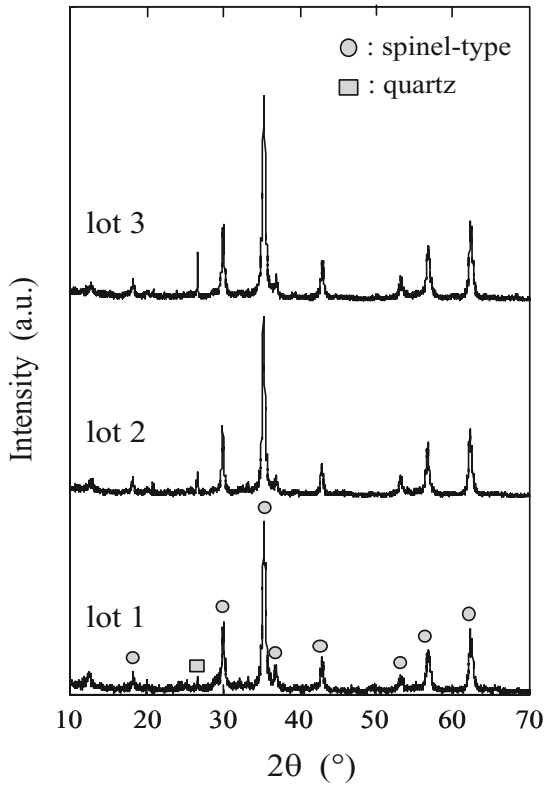

Figure 4 XRD patterns of lot 1–3 dusts after hydrothermal treatments in the presence of 5 M NaOH solution with a solid/liquid ratio of 1/30 at 373 K for 24 h.

lot 1–3 dusts were treated in the presence of 5 M NaOH solution with solid / liquid ratio of 1/30 at 373 K for 24 h. Fig. 4 shows XRD patterns of the treated dusts, exhibiting that the dominant phase is the spinel-type compound, accompanied by a small amount of quartz after the treatment. The TEM image, furthermore, revealed that most of the spinel-type nanocrystals were extracted by the dissolution of the matrixes as seen in Fig. 5. The H_2S sorptive capacities of the dust before and after the NaOH treatments were measured. The NaOH treatments notably resulted in the enhancement of the H_2S sorptive properties, as listed in Table II. These indicate that the H_2S sorptive properties of the dusts are attributable to the spinel-type nanocrystals.

Furthermore, lot 1–3 dusts were treated under various conditions in the presence of 5–15 M NaOH solutions. From the results, the H_2S sorptive capacities of some treated dusts, in which the crystalline spinel-type

TABLE II H_2S sorptive capacities of cupola dusts before and after hydrothermal treatments with 5 M NaOH

	H_2S sorptive capacity (g·g^{-1})		
Hydrothermal treatment	Lot 1	lot 2	lot 3
Before	0.081(4)*	0.072(4)	0.095(5)
After	0.253(9)	0.225(10)	0.242(11)

*A numbered in a paranthesis denotes an experimental error

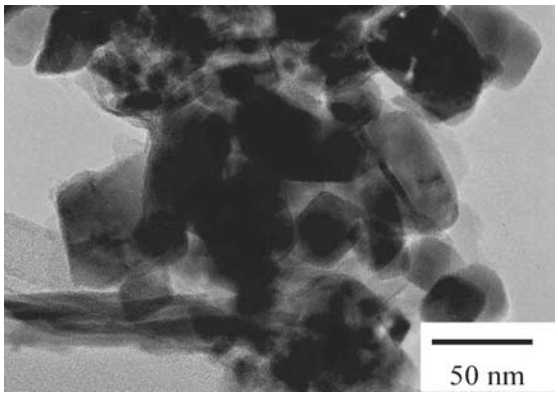

Figure 5 TEM image of lot 1 dust after hydrothermal treatment in the presence of 5 M NaOH solution with a solid/liquid ratio of 1/30 at 373 K for 24 h. Opaque particles are spinel-type nanocrystals.

compounds only remained, further increased, and the maximum amounted to about 0.33 $g \cdot g^{-1}$. The high H_2S sorptive capacities are comparable to those of other H_2S sorbents on the market such as $ZnFe_2O_4$ (Johnson Matthey, London, U.K.) and Fe-based compound (Nissan Girdner Catalyst, Tokyo, Japan), whose H_2S sorptive capacities were measured to be 0.29 and 0.27 $g \cdot g^{-1}$, respectively.

3.4. Sorptive mechanism

The H_2S sorptive capacities of NaOH-treated dusts were examined with respect to the chemical composition, the specific surface area and the solubility in order to clarify the sorptive mechanism of the spinel-type nanocrystals. Fig. 6 shows the relation between the total content of Mn, Zn and Fe in the NaOH-treated dust analyzed by an XRF technique and the H_2S sorptive capacity to the treated dust. There seemed a tendency that the H_2S sorptive capacity increased with increasing total metal content in the NaOH-treated dust. However, the clear correlation between the total metal content and the H_2S sorptive capacity was not observed in lot 1 and 2 dusts. Then, the relations between the fractions of Mn, Zn and Fe to the total metal content and the H_2S sorptive capacity were

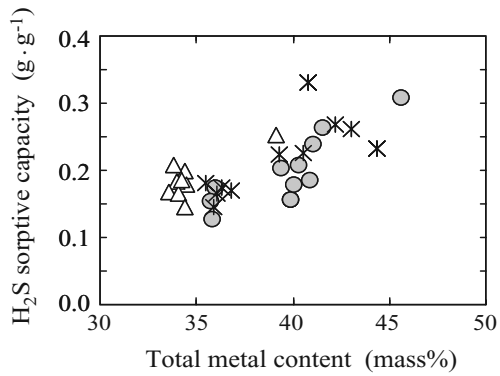

Figure 6 Relation between the total content of Mn, Zn and Fe in the NaOH-treated dust under various treatment conditions and the H_2S sorptive capacity. Symbols, ∗, △ and ○, represent lot 1, 2 and 3 dusts, respectively.

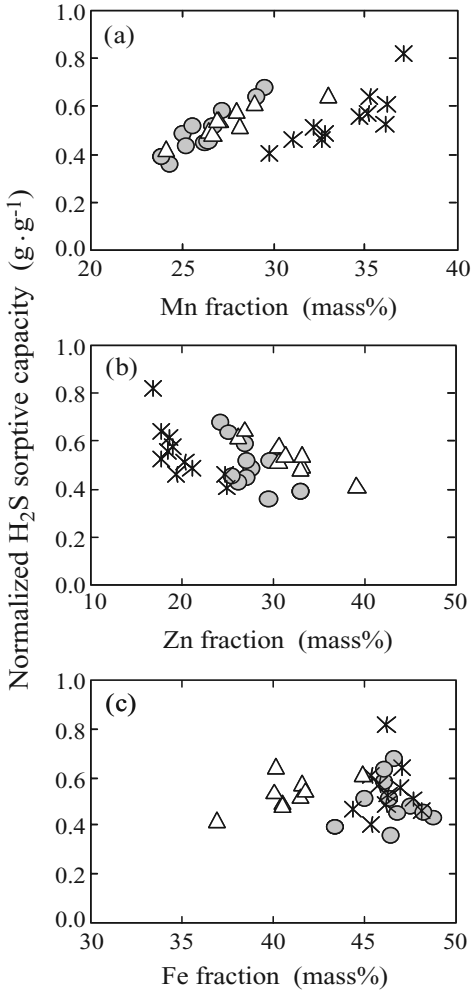

Figure 7 Relations between the respective metal fractions of (a) Mn, (b) Zn and (c) Fe to the total metal content in the NaOH-treated dust and the normalized H_2S sorptive capacity to the total metal content. Symbols, ∗, △ and ○, represent lot 1, 2 and 3 dusts, respectively.

examined to further clarify factors which contribute to the H_2S removal. The H_2S sorptive capacity to the treated dust, i.e. the H_2S sorbed weight per 1 g of the NaOH-treated dust, was normalized to the H_2S sorptive capacity to the total metal content, i.e., the H_2S sorbed weight per 1 g of total metal contained in the treated dust, because the spinel-type nanocrystals act as a sorbent. The resulting relations between the respective metal fractions to the total metal content in the NaOH-treated dust and the H_2S sorptive capacity to the total metal content are shown in Fig. 7. The normalized H_2S sorptive capacity remarkably increased with a higher content ratio of Mn, whereas it decreased with a higher content ratio of Zn, and a content ratio of Fe had no impact on the capacity. Namely, these results mean that the fractions of Mn and Zn in the spinel-type nanocrystals influence the H_2S sorptive capacity.

The H_2S sorptive capacity as a function of the specific surface area was examined, because specific surface area of a porous material affects its removal characteristics. However, the clear relation between the specific surface

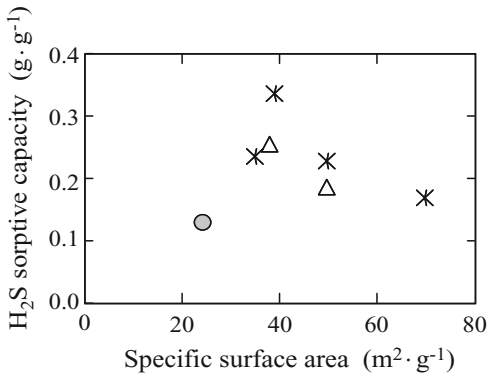

Figure 8 Relation between the specific surface area of the NaOH-treated dust under various treatment conditions and the H_2S sorptive capacity. Symbols, ∗, △ and ○, represent lot 1, 2 and 3 dusts, respectively.

area and the H_2S sorptive capacity of the NaOH-treated dust was not observable, as shown in Fig. 8.

Next, the solubility of the NaOH-treated dust into water was examined on the basis of the fact that the H_2S sorptive property appears in existence of water vapor, as shown in Fig. 3. The H_2S sorptive capacity of the NaOH-treated dust was plotted versus the total concentration of Mn, Zn and Fe released from the treated dusts in the water, as shown in Fig. 9. The clear correlation between them was observed, exhibiting that the H_2S sorptive capacity increased with solubility. Thus, the solubility of the NaOH-treated dusts was noticed in order to clarify which components in the spinel-type nanocrystals affect the H_2S absorptive property. Fig. 10 shows relations between the fractions of Mn, Zn and Fe to the total metal content in the NaOH-treated dust and the solubility of the treated dust. The solubility increased with increasing content ratio of Mn, whereas it decreased with increasing content ratio of Zn, and did not rest on a content ratio of Fe. This aspect was similar to that observed in Fig. 7. It was, therefore, found that Mn and Zn fractions in the spinel-type nanocrystals influenced the H_2S sorptive property and the solubility of the NaOH-treated dust predominantly consisting of the spinel-type nanocrystals.

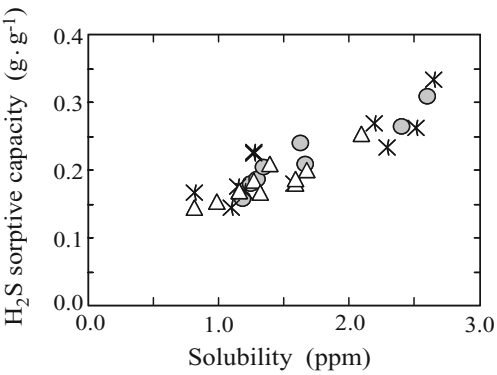

Figure 9 Relation between the H_2S sorptive capacity and the solubility of the NaOH-treated dust. The solubility is represented by the total concentration of Mn, Zn and Fe released from the NaOH-treated dust in the deionized water. Symbols, ∗, △ and ○, represent lot 1, 2 and 3 dusts, respectively.

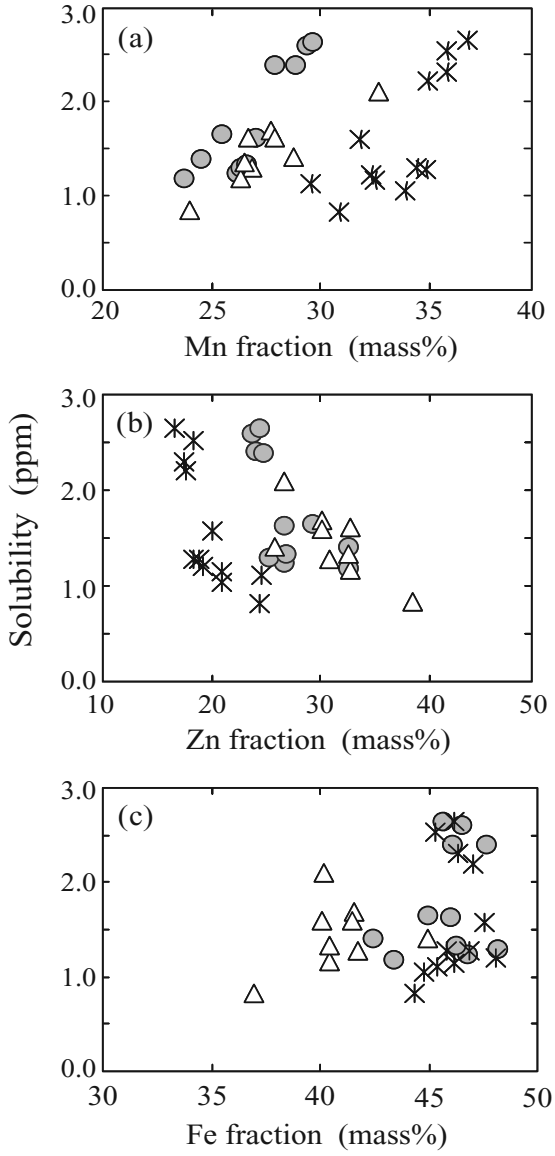

Figure 10 Relations between the respective metal fractions of (a) Mn, (b) Zn and (c) Fe to the total metal content in the NaOH-treated dust and the solubility. The solubility is represented by the total concentration of Mn, Zn and Fe released from the NaOH-treated dust in the deionized water. Symbols, ∗, △ and ○, represent lot 1, 2 and 3 dusts, respectively.

The results drive the sorptive mechanism for H_2S as follows. H_2S is easily dissolved in the water adsorbed on the surface of the spinel-type nanocrystals, and react with metal ions released from the spinel-type nanocrystals.

$$(-MO)_{solid} + H_2S + H_2O \rightarrow M^{2+} + O^{2-} + S^{2-}$$
$$+2H^+ + H_2O \rightarrow MS + 2H_2O$$

This mechanism was supported by the fact that new broad peaks at around $2\theta = 28$, 47 and 55°, which were assigned to transition metal sulfide compounds such as MS (M = Mn, Fe and Zn), appeared on the XRD pattern of the NaOH-treated dust after contactiong with H_2S gas as shown in Fig. 11.

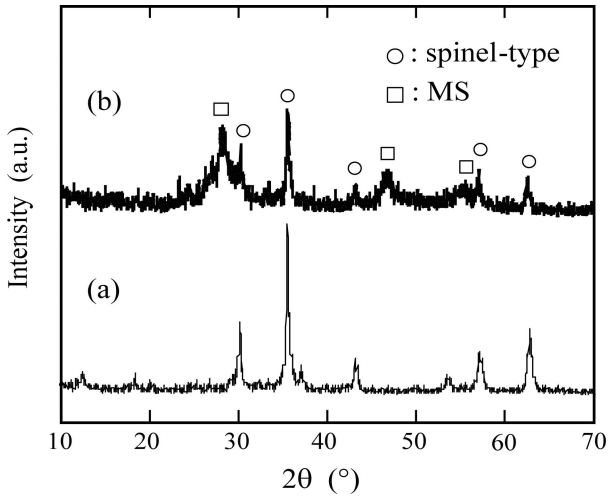

Figure 11 XRD patterns of 5 M NaOH-treated lot 1 dust (a) before and (b) after contacting with H_2S gas. MS represents transition metal sulfide compounds such as MnS, FeS and ZnS.

4. Conclusions

The investigation on the H_2S sorptive property of the cupola dust leads to the following conclusions, through the characterizations such as chemical composition, crystalline phase, specific surface area, sorptive capacity and water solubitity. The spinel-type nanocrystals, $(Mn_xZn_{1-x})(Mn_yFe_{1-y})_2O_4$ solid solutions identified as a main crystalline phase in the dust, act well as a desulfurization sorbent at room temperature in existence of water vapor. The water adsorbed on the surface of the spinel-type nanocrystals was considered to play a role as a sorptive field, where H_2S gas dissolved in the water reacts with metal ions released from the spinel-type nanocrystals. The reactivity increases with increasing content ratio of Mn in the spinel-type nanocrystals, whereas it decreases with increasing content ratio of Zn. Namely, the amounts of Mn and Zn in the spinel-type nanocrystals are effective factors for the H_2S sorptive property of the cupola dust. The NaOH-treated cupola dust with the high H_2S sorptive capacity, comparable to those of H_2S sorbents on the market, was expected to be usable as an H_2S sorbent at room temperature.

Acknowledgment

This work was partly supported by the Okayama University 21st Century COE Program "Strategic Solid Waste Management of Sustainable Society".

References

1. Z. YAO, C. TAMURA, M. MATSUDA and M. MIYAKE, *J. Mater. Res.* **14** (1999) 4437.
2. C. TAMURA, Z. YAO, F. KUSANO, M. MATSUDA and M. MIYAKE, *J. Ceram. Soc. Jpn.* **108** (2000) 150.
3. M. MIYAKE, C. TAMURA and M. MATSUDA, *J. Am. Ceram. Soc.* **85** (2002) 1873.
4. T. HENMI, *Soil Sci. Plant Nutr.* **33** (1987) 517.
5. C. LIN and H. HSI, *Environ. Sci. Technol.* **29** (1995) 1109.
6. M. PARK and J. CHOI, *Clay Sci.* **9** (1995) 219.
7. C. AMRHEIN, G. HAGHNIA, T. KIM, P. MOSHER, R. GAGAJENA, T. AMANIOS and L. TORRE, *Environ. Sci. Technol.* **30** (1996) 735.
8. Y. SUYAMA, K. KATAYAMA and M. MEGURO, *J. Chem. Soc. Jpn.* **1996** (1996) 136.
9. X. QUEROL, A. ALASTUEY, A. SOLER and F. PLANA, *Environ. Sci. Technol.* **31** (1997) 2527.
10. X. ZHAO, G. LU and H. ZHU, *J. Porous Mater.* **4** (1997) 245.
11. W. MA, P. W. BROWN and S. KOMARNENI, *J. Mater. Res.* **13** (1998) 3.
12. H. TAKAHASHI, T. MARUTA, K. SAKAE and M. KASAHARA, *J. Soc. Inorg. Mater. Jpn.* **5** (1998) 200.
13. T. HATTORI, M. MATSUDA and M. MIYAKE, *J. Ceram. Soc. Jpn. Suppl.* **112** (2004) S1347.
14. M. C. WOODS, S. K. GANGWAL, D. P. HARRISON and K. JOTHIMURUGESAN, *Ind. Eng. Chem. Res.* **30** (1991) 100.
15. M. KOBAYASHI, H. SHIRAI and M. NUNOKAWA, *Energy and Fuels* **11** (1997) 887.
16. M. A. AHMED, L. ALONSO, J. M. PALACIOS, C. CILLERUELO and J. C. ABANADES, *Solid State Ionics* **138** (2000) 51.
17. E. GARCIA, J. M. PALACIOS, L. ALONSO and R. MOLINER, *Energy and Fuels* **14** (2000) 1296.

Received 9 March 2005
and accepted 10 August 2005